SECTION 7

ANALYSIS OF MULTISPECTRAL IMAGES SIMULATING ERTS OBSERVATIONS

by

Nicholas M. Short & Norman H. MacLeod
Earth Observations Branch
Goddard Space Flight Center
Greenbelt, Maryland

INTRODUCTION

In response both to the anticipated desires of the User Community for simulated imagery prior to launch of the first Earth Resources Technology Satellite (ERTS-A) and to the need for such products suited to scientific and technological evaluation at Goddard, a simulation study of selected aircraft- and spacecraft-acquired images was initiated in 1971 within the Earth Observations Branch at Goddard Space Flight Center. The principal modes of simulation include: first, areas of coverage comparable to ERTS, that is, approximately 183 km (100 nm) on a side; second, spatial resolutions within these images similar to ERTS (namely, about 100 meters for the two ERTS sensor systems at optimum signal to noise ratios); third, spectral responses analogous to that expected from each channel on both the Return Beam Vidicon (RBV) and Multispectral Scanner (MSS), leading to production of photographic images that should appear similar to those representing each band in the two sensors (spectral response curves for each band are shown in Figure 1); and, fourth, runthroughs of several analytical techniques, such as color density slicing, color additive viewing, and computer-generated reflectance and surface temperature maps, by which ERTS data can be analyzed, interpreted, and applied.

The two regions involved in the simulation study are Wyoming - selected as typicalof a semi-arid surface dominated by geological features and considerable topographic variation, and the Chesapeake Bay region around Washington, D.C. and eastward - chosen as characteristic of a humid climatic environment, dominated by vegetation, flat, and bounded by a marine coastline.

NIMBUS STUDIES

The first step in these simulation studies began with examination and analysis of certain Nimbus meteorological satellite images. Nimbus I, a short-lived satellite with an eccentric orbit, produced many intriguing pictures of the Earth's surface at resolutions of a kilometer or better near perigee. The scene depicted in Figure 2 represents one of the finest examples of high altitude synoptic imagery obtained from unmanned satellites to date. Comparison of the image - covering parts of southwest Wyoming, northwest Colorado, northeast Utah, and eastern Idaho - with the geological map of the same area shows that nearly all major structural and topographic units can be readily recognized. The light, highly reflective basins stand out in sharp contrast to the uplifted mountains which appear dark in the image because of the much more extensive vegetation cover - mainly thick grasses and conifers. These contrasts can be further enhanced by converting the photographic grey levels into colors by use of a TV color density slicing system (Figure 3). In general, the lack of high resolution in Nimbus photos is offset by these distinct differences in contrast that allow ready recognition of major vegetation groups and moisture variations on a regional, synoptic scale.

Dr. V. Salomonson of the Meteorology Branch at Goddard has produced a surface temperature distribution map of the entire state of Wyoming from emitted thermal radiation at 11.5 micrometers as dectected by the THIR or Temperature-Humidity Infrared Radiometer on Nimbus IV. This channel is similar to the thermal channel peaked between 10.4 and 12.6 micrometers planned for ERTS-B, although the THIR resolution of 8 kilometers is much less than that of about 300 meters being designed for ERTS-B. A schematic relief map of Wyoming appears in Figure 4c. This should be compared first with a computer-generated map of THIR-sensed data for the entire state obtained during a daytime pass on July 4, 1970 (Figure 4b). Color codes show the surface temperature range after appropriate corrections are made. It is immediately evident that, again, most of the principal topographic features within the state are well defined by the temperature variations. These variations are accentuated primarily by the pronounced relief or differences in elevation between the relatively cool uplands and the hotter intermontane basins. Broad patterns coincident with structural uplifts within the basins or with major drainage systems can even be discerned. However, when THIR looks at this same surface at night (Figure 4a), on the same July 4th, the temperature distribution pattern becomes far less recognizable when attempts to correlate with topography are made - although the general positions of basins and mountains are crudely defined.

WYOMING AIRCRAFT SIMULATIONS

Let us turn now to efforts to simulate ground scenes of the same general size or areal extent and spatial resolution as expected from ERTS. Invaluable experience pertinent to this was already available through the studies of Gemini and Apollo orbital photography made by Lowman, Abdel-Gawad, and others. The chief conclusions reached by these workers and by many other specialists in remote sensing are that such small scale (that is, large areas of coverage) images have a tremendous inherent capability for providing synoptic overviews of extensive sections of the Earth's surface and that many individual ground features at or near the limits of resolution could be successfully identified by classification techniques based on diagnostic spectral and spatial characteristics or signatures.

Rather than retread the path laid out by these orbital photography experts, we have followed a somewhat different approach. Largely through the ingenuity of R. Sabatini and others of the Allied Research Corporation supporting Nimbus, a simple technique for progressively degrading images with initially high resolutions has been developed. In its essence, this technique involves reprinting a photograph at various sizes smaller than the original, photographing these again as is, and then enlarging the variously reduced negatives to a single constant size before final printing. Control in the process is maintained through use of a grey level scale and a three-bar resolving-power target that aids in calculating new resolutions.

As a first test of the method, a remarkable photomosaic of the Los Angeles area made at an initial scale of 1: 400,000 by Aero Service Corp. of Philadelphia, Pa from over 10,000 individual aerial photos was systematically degraded from an initial ground resolution of about 15 meters (Figure 5a; reduced through steps of 30 and 55 meters) through steps of 25, 50, 100, and 200 meters (using an 8 x 10 print) (Figure 5b). Two conclusions are strikingly obvious. First, regardless of resolution, all the first- and second-order land features are visible and generally identifiable at all these resolutions. The various mountain units, some major geological structures expressed topographically (including the San Andreas fault zone), most larger drainage systems, and the bigger agricultural fields remain evident in the lower resolution renditions. Second, however, useful and sometimes essential details relevant to mapping or to feature identification are lost in the low resolution (e.g., 200 meter) image. This is best demonstrated by examining the cultural features present in the Los Angeles basin, preferably with the aid of a magnifying glass.

We have now tried essentially the same type of progressive degradation on an area within central Wyoming (Figure 6) whose dimensions approximate that of a single ERTS field of view or frame reproduced photographically. The region covered centers on the Wind River basin surrounded by uplifted mountain blocks some 1500 to 3000 meters higher in elevation. In the Nimbus TV imagery, these uplifts appear significantly darker in a processed photofacsimile. In an Aero Service-produced composite photomosaic at a 1:250,000 scale (put together from more than 12,000 aerial photos in a 1952 flight sequence), shown in Figure 7a, it is very hard to spot the uplifts or the deformed structures within the basin. This is one of the weaknesses associated with this type of photomosaic - in which the aerial surveying plane usually flew around high noon to minimize shadows and some contrasts are later removed by dodging during preparation of the mosaic. This tends to obscure some of the structural and topographic relationships that make a synoptic view so attractive for interpreting large units of the Earth's crust. Still, careful examination of the photograph shown in Figure 7b, degraded to about 130 meters resolution, reveals that many critical details have remained detectable. When degraded to 285 meters resolution (Figure 7c), most major elements of interest in the scene are still recognizable and can be adequately mapped. What is sacrificed in this scene are specific details of secondary drainage, individual rock units, cultural layouts in towns, and the like; however, changes in tonal patterns as seen under magnification can sometimes be interpreted to correctly identify these features.

On October 21, 1971, a U-2 flight over essentially the same area of central Wyoming was conducted for the first co-author by NASA Ames Research Center. The aircraft carried four Vinten cameras, three of which contained film-filter combinations designed to simulate the ERTS RBV sensor system. Each camera produced individual pictures about 26 km (14 nm) on a side, with slight overlap and sidelap among photos in the flight lines. The effective ground resolution is between 15 and 20 meters. We have prepared an uncontrolled photomosaic from some 54 individual frames using the red band images (Figure 8). Because the red band optimizes contrasts in a scene dominated by geologic features, some of the structural, topographic, and geomorphic features scarcely discernible in the Aero Service mosaic are more readily picked out in the U-2 composite mosaic.

Instead of decreasing the resolution of the entire scene, a sequence of degradations was carried out on a single 26 km frame. The area selected is in the vicinity of Ocean Lake near the northwest corner of the Wind River basin. An Aero Service photomosaic that covers this area appears in Figure 9a and an undegraded (resolution about 18 meters) U-2 frame extending over much the same area is shown in Figure 9b. Figure 10a illustrates the scene at a resolution of about 45 meters. As before, most of the essential information remains intact. When degraded to 100 meters, the principal loss of information again is in the fine structure of drainage systems, rock and soil distribution, etc. But the overall synoptic aspects of the scene continue to stand out in their proper context.

This same scene can also be examined through different regions of the photographic spectrum. The simulated green band view (Figure 11a), when compared to the red band view (Figure 11b), discloses one evident difference. The photographic contrasts between various areas of rock and soil and between agricultural fields (most of which were harvested and barren by October 21) are distinctly less in the green than in the red. On the other hand, sediment in the lake is evident only in the green band photo. Next, compare the IR band (Figure 11c) with the red band. Contrasts within the cultivated areas are reduced - mainly because most of the crops are gone. During growing season the IR band could show stronger contrasts than in the red band. Moisture variations in the desert wastes south of the lake show up well in the IR and also in the red bands but less so in the green. Another example appears in Figures 12a, b, and c. Once more, maximum contrast, and hence scene definition, occurs in the red band. Some contrasts are evident in the IR but the green band photo looks more or less washed out and rather dark.

These observations agree with Lowman's conclusions for desert areas seen in the SO-65 Apollo 9 experiment. The explanation is straighforward: In Wyoming, most of the surface in the basins is dominated by rocks and soils whose colors range from reds to browns to grays to buff. As viewed within the visible red wavelength region, color variations on such surfaces should lead to large photo density contrasts. Sparsity of vegetation causes minimal changes in the green and IR band photos.

STUDIES IN THE CHESAPEAKE BAY (CARETS) REGION

Lets switch our attention now to simulation studies in the eastern United States. Figure 13 presents a synoptic photomosaic of the Chesapeake Bay region, enclosing an area about 220 km (120 nm) across the view and 275 km (150 nm) from top to bottom. This picture was constructed from over 110 individual red band frames obtained during a U-2 flight on September 15, 1971. The U.S. Department of Agriculture has completed a similar photomosaic with the green band photos from this flight. Comparison of the two products, at nearly equivalent scales, reveals a sharper contrast among the major land features - mostly farm and forest plots - within the green band. This is observed repeatedly in individual frames covering rural areas in the Delmarva peninsula.

Figure 14a, b, and c consists of the green, red, and IR band photos of an area which includes Goddard Space Flight Center, the Beltway northeast of Washington, D.C., and the Washington-Baltimore Parkway. Again, the heavily vegetated areas, such as those within the Beltsville Agricultural Experiment Farms, show up best in the green band. But because of the extensive cultural - or suburban - development in this area and the presence of many sand and gravel pits, the contrast seems even greater in the red band panorama. In the IR band photo, the overall tone of the picture is bright, with subdued contrast except for the water backed up behind a dam on the Pawtuxent River north of Laurel, Maryland. Towns and other cultural features are hard to distinguish from surrounding vegetation at first glance. This particular scene indicates the effects in the IR of a suburban environment in which everyone is still trying to keep his lawn and shrubery in growth as late as September 15. The uniform brightness, then, gives a different impression than that of the IR band views of the farmlands in eastern Maryland, where considerable harvesting had already altered the growth pattern by then.

A red band U-2 frame that covers an area in Maryland's eastern shore where Highway 50 crosses the Choptank River is reproduced in Figure 15a. Ground truth data for many of the features clustered along the highway in this section were obtained by N. H. MacLeod. Figure 15b shows a reconstructed false color IR image, produced on an I^2S color additive viewer, which should approximate the type of color photo that will be produced routinely from the three RBV images on ERTS. In this image, the green band is projected through a blue filter, the red through a green, and the IR band through a red filter. As expected, the forest areas reappear as dark red, the growing field crops as lighter red, and fallow fields, excavations, and town areas mainly as shades of blue or green.

In mid-October, 1971 the multispectral scanner developed by Warren Hovis of the Earth Observations Branch at Goddard for ERTS simulation was flown on an aircraft at an altitude of 2500 meters over this same Choptank River area and other parts of the Delmarva peninsula. The photo imagery was produced by converting the analog voltage data recorded on magnetic tape into video signals processed through an electron beam recorder into a picture. The four channel MSS image obtained over a strip along Highway 50 appears in Figure 16. The numbers refer to individual identified features, labelled in Figure 17, within which photo densities of corresponding areas in each band image were measured. It should be stressed that these measurements, plotted graphically in Figure 17, cannot be considered as quantitative owing to non-calibration of either the raw MSS data or photographic reproduction and to the relative simplicity of the densitometer used. Note too that noise has not been removed, as is evident in channel 4. The signature data are thus only approximations of the kinds of results expected from the ERTS MSS system.

The following generalizations can be summarized from interpretations made on Figures 16 and 17:

1) The images produced from the first two channels - the visible green and red bands - are, in general, similar to one another in terms of the densities associated with specific feature categories.

2) The two IR channels are, to a lesser extent, also similar to one another.

3) The two pairs of channels - visible and IR - produce images that are distinctly different from one another.

4) The signatures of the same feature classes appear to be reproducible throughout the scene, as suggested by the very similar density values obtained for the two separate mixed hardwood stands and the two fields containing old hay.

5) Ambiguities about whether bright (light grey tones) areas in the visible channels represent fallow fields or growing crops are clearly resolved by the IR channels.

6) At the resolution of the MSS images - about 10 meters - the identification of dark-toned areas in the first two channels as forests of taller trees is confirmed by the third channel, in which tree canopy patterns give rise to a distinctive texture.

Now, to counter the impression that two of the four MSS channels may seem redundant, look at the last illustrations. The U-2 RBV-simulated photographs for part of the Atlantic coastline along Assateague Island (Maryland-Delaware) appear in Figure 18. The MSS counterpart for the offshore bar area is shown in Figure 19. Close inspection of patterns representing beach sand and dune sand distributions and vegetation along drainage paths or in tidal marshes, etc. will reveal that channels two and four add significant new information in relation to channels one and three. Visual differences in tone or grey level, not too apparent to the eye at first glance, prove larger than suspected when areas are densitometered and channel density levels are ratioed.

SUMMARY

In conclusion, these main points are reiterated:

First, even at resolutions around 100 meters, the synoptic character of diverse ground scenes extending over wide areas remains strongly expressed and, in some respects, is emphasized by loss or reduction of details.

Second, each band on the RBV or MSS sensors appears to have a useful function for certain specific tasks. Thus, on one type of land surface, one visible band may be superior to another but with the converse true in another region with different land surface types.

Lastly, interesting and exciting though these simulation images may be, they'll pale and be forgotten the day we begin to get the real products from ERTS itself.

ACKNOWLEDGEMENTS

We are particularly grateful to Mr. Ronald Sabatini and Mr. Walter Ahlin of the Allied Research Corporation for their generous assistance in preparing many of the illustrations appearing in this paper.

SPECTRAL RESPONSE FOR ERTS-A

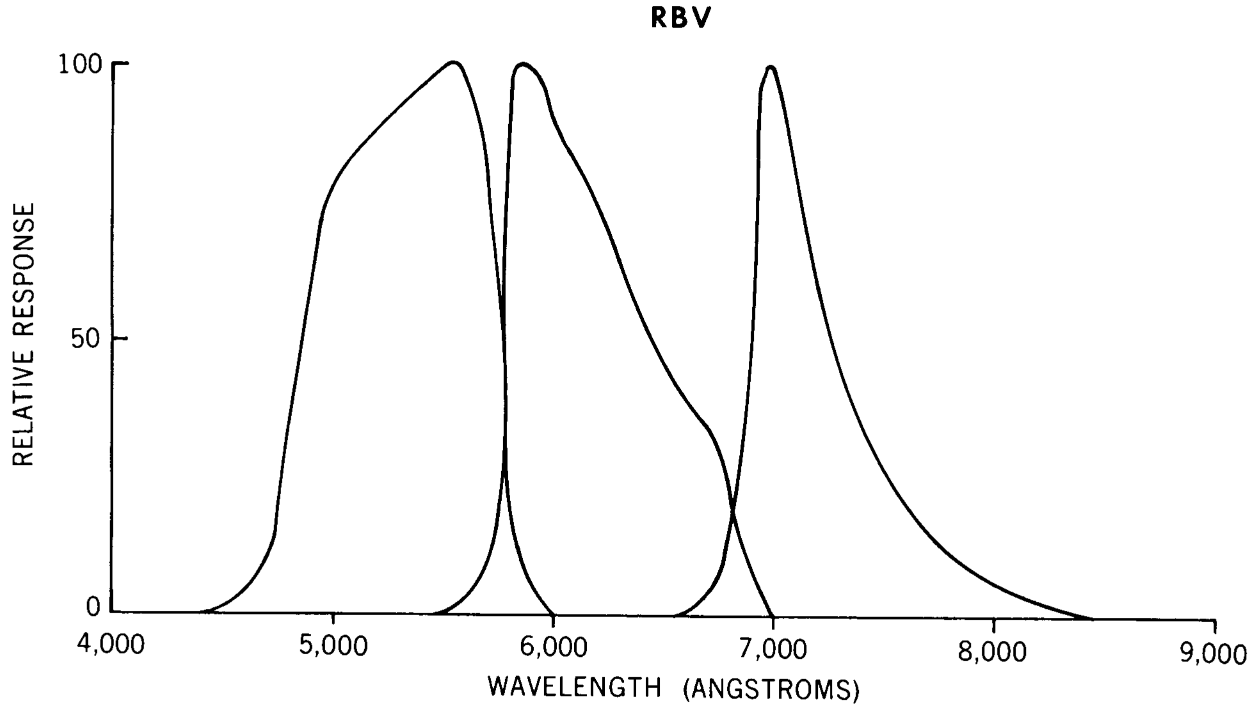

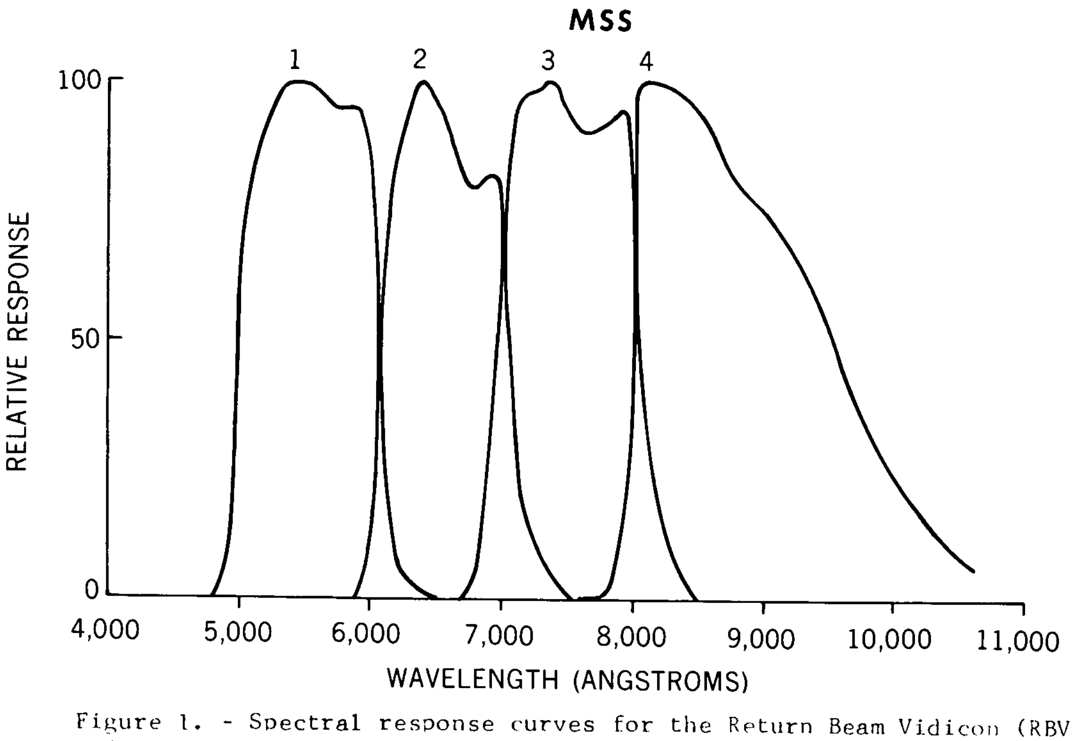

Figure 1. - Spectral response curves for the Return Beam Vidicon (RBV) (calculated) and Multispectral Scanner (MSS) (measured) sensors on ERTS-A

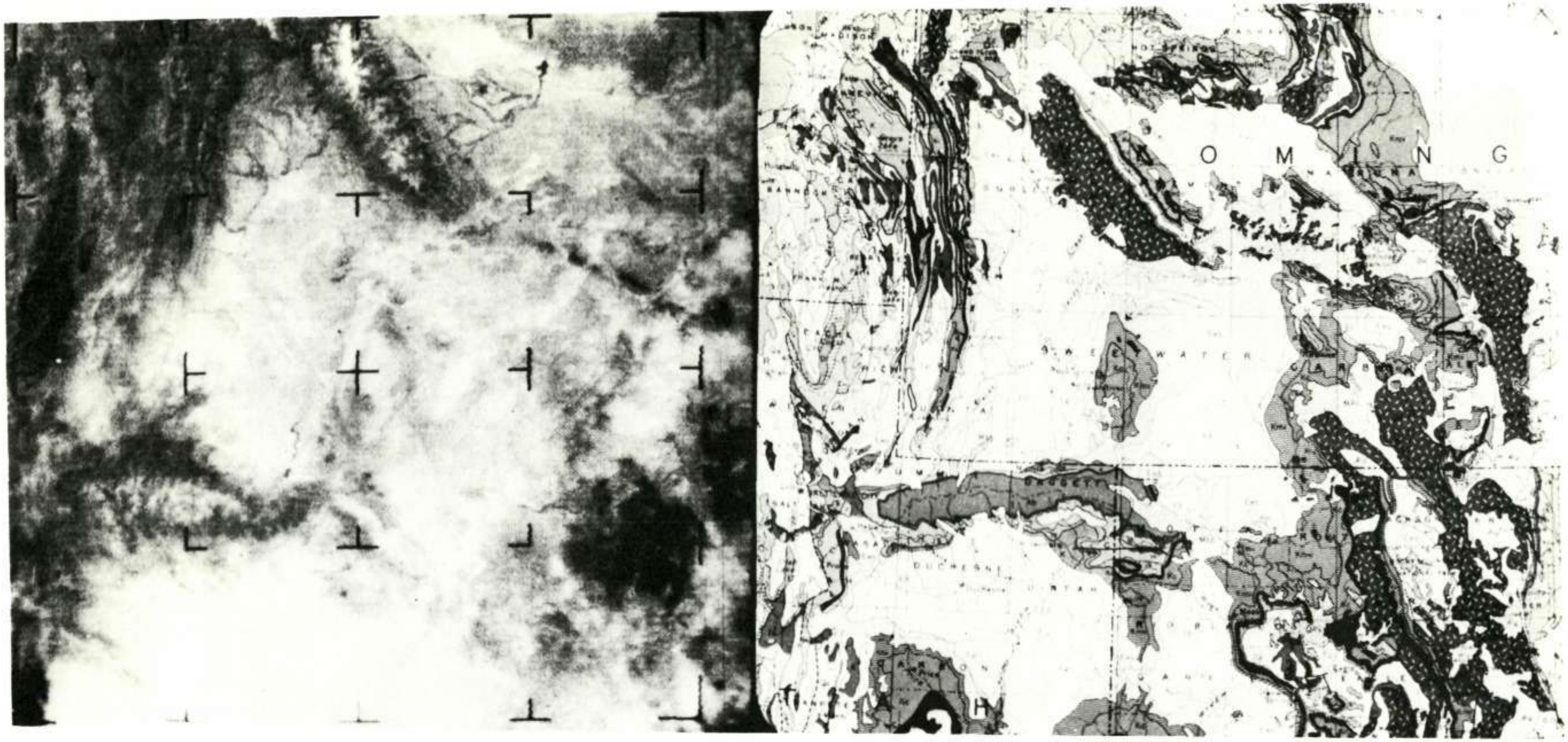

Figure 2. - Left: Nimbus I AVCS (television) photofacsimile of southwestern Wyoming, northwestern Colorado, and northeast Utah taken on September 4, 1964 (orbit 109) from an altitude of approximately 890 km. The large, light area in the center is the Green River basin; a similar area to the south is the Uinta basin. The Wind River mountains appear in the top center, the Wyoming-Hoback Ranges to the left of these, and the east-west Uinta Range on the lower left below center. Right: A geological map (from U.S. Geological Survey map of the U.S.) showing the region covered by the Nimbus I image.

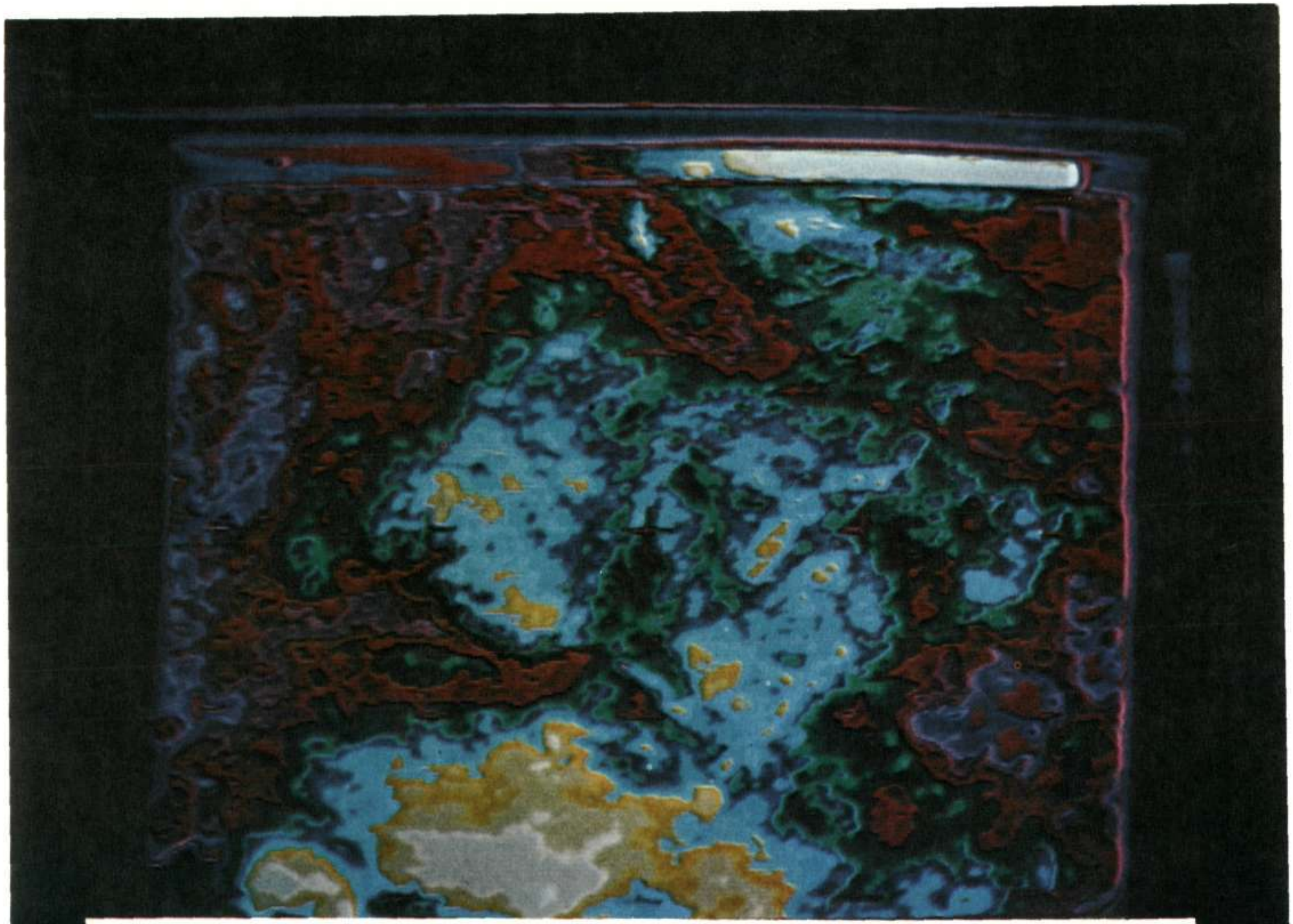

Figure 3. - The Nimbus I image shown in Figure 2, left as rendered in a color disolay by a Ṡpatial Data Systems Model 703-32 Datacolor unit. As translated by TV scanning of the black and white image, very light greys appear as yellows, followed by a sequence for darkening grey levels through blues, greens, dark olive, red, mauve, and bluish-purple.

NIMBUS 4 THIR 10.5–12.5 μm OBSERVATIONS OVER WYOMING

JULY 4, 1970

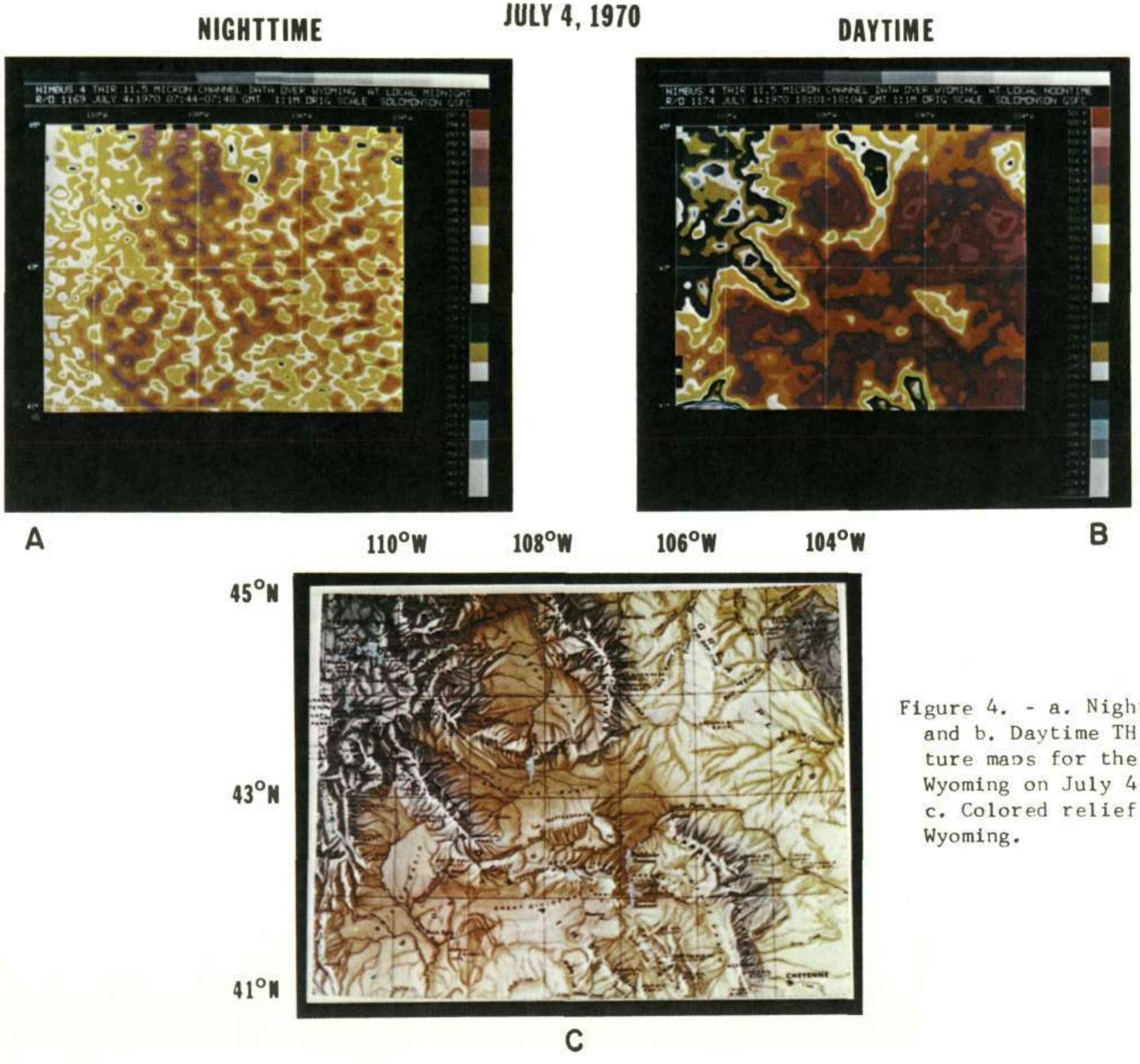

Figure 4. - a. Nighttime THIR and b. Daytime THIR temperature maps for the surface of Wyoming on July 4, 1970. c. Colored relief map of Wyoming.

(A)
Aerial Photomosaic of Los Angeles and Mojave Desert Areas

(B)
Degraded Image of (A)
Resolution is approx. 200 meters.

PRODUCED BY ALLIED RESEARCH ASSOCIATES, CONCORD, MASS.

Figure 5. - a. Composite aerial photomosaic of the Los Angeles basin - Mojave desert areas of California; San Gabriel Mountains in the center. The resolution of the original 8 x 10 inch photo before reduction to illustration size is about 30 meters; as reproduced here it is about 55 meters. b. Same scene reduced in resolution to approximately 200 meters; or about 350 meters as printed.

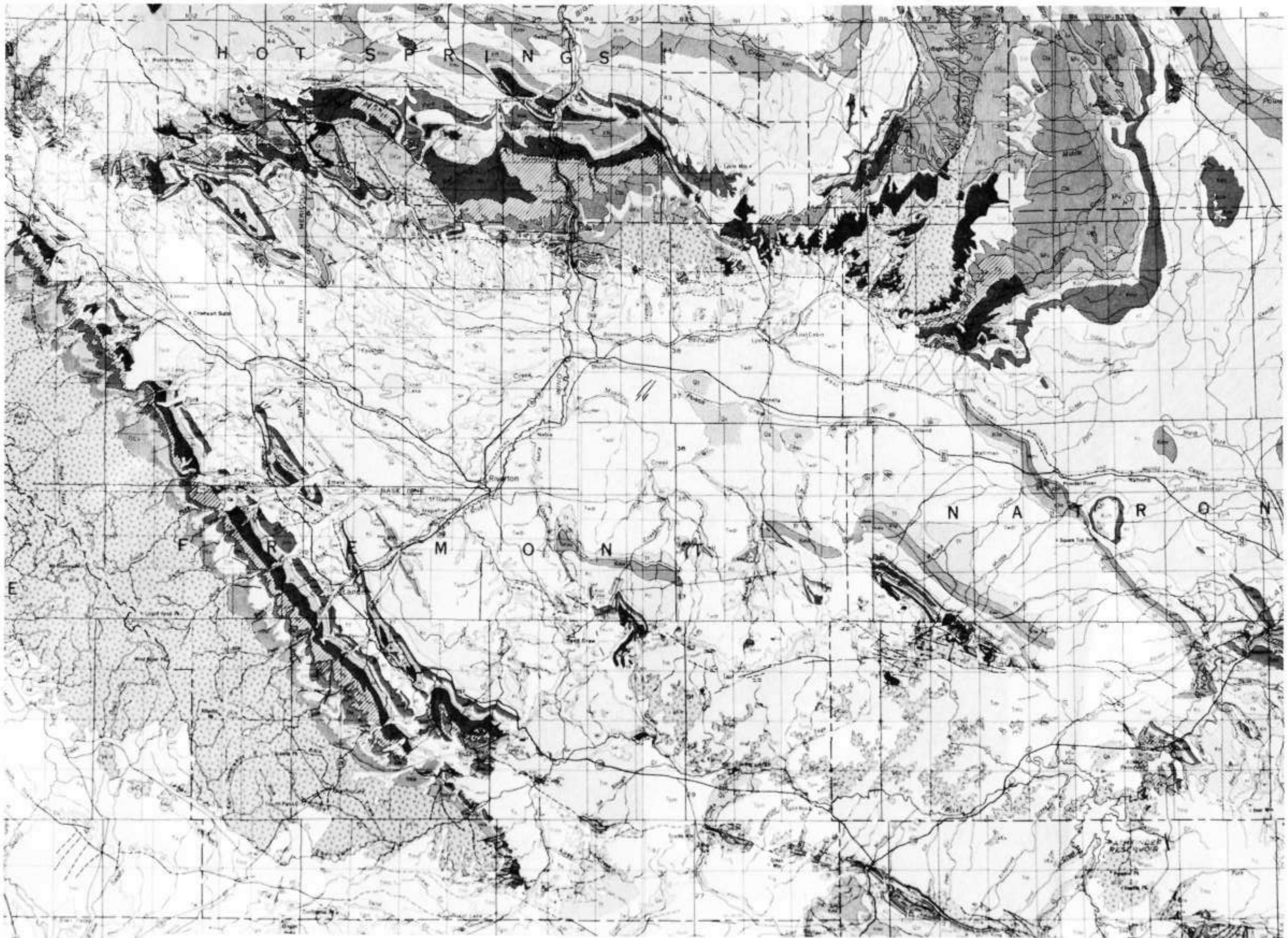

Figure 6. - Part of the geologic map of Wyoming showing the Wind River basin (central Wyoming), the Wind River Mountains (left), the Owl Creek and Bridger Mountains (top), and the Rattlesnake Mountains (below and left of word Natrona); compare with Figures 7 and 8.

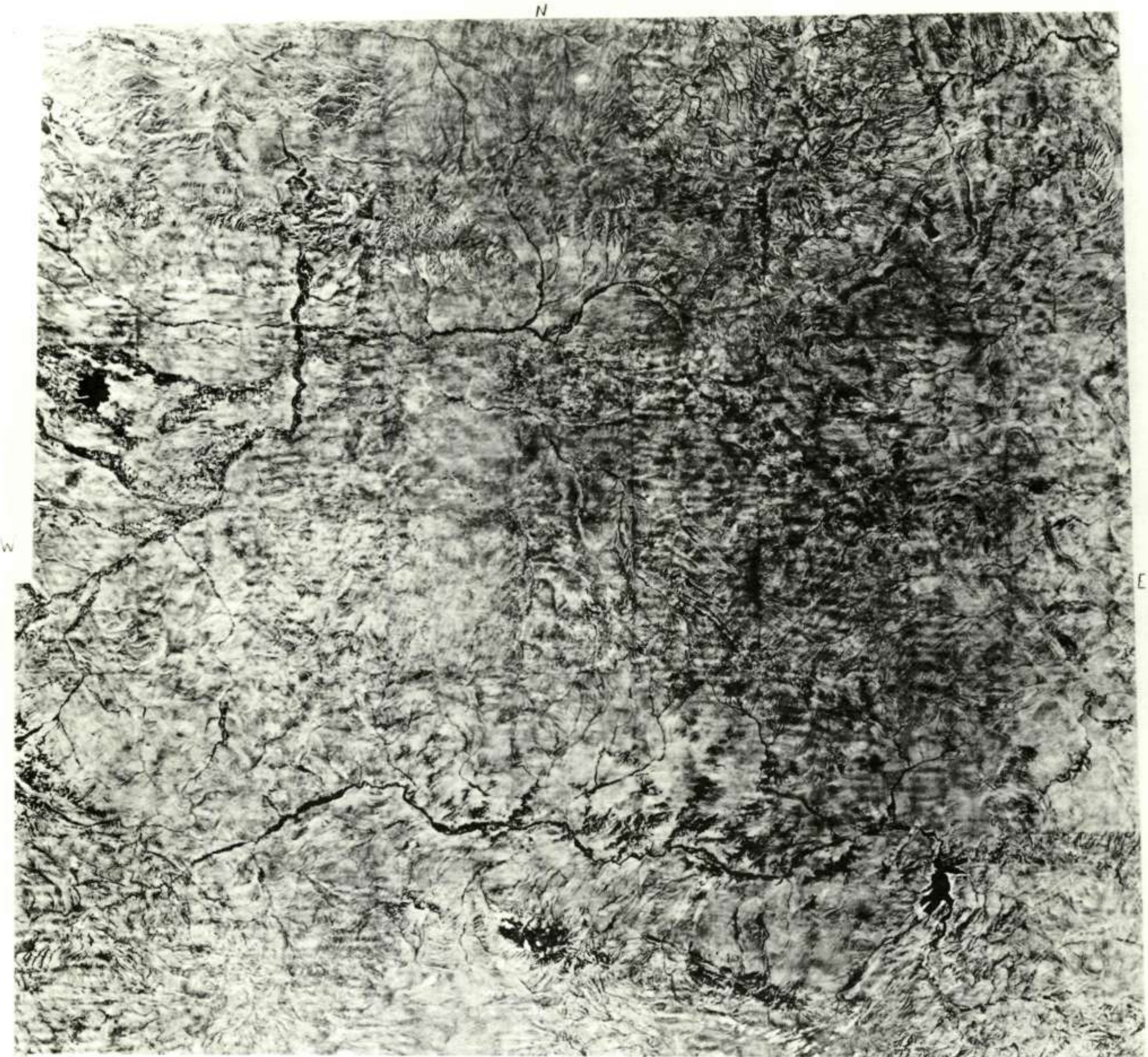

Figure 7a. - A composite photomosaic of the Wind River basin region; produced by Aero Service, Inc. at an initial scale of approximately 1:425,000 and a resolution of about 15 meters. As reduced in this illustration, resolution is estimated to be near 60 meters.

a.

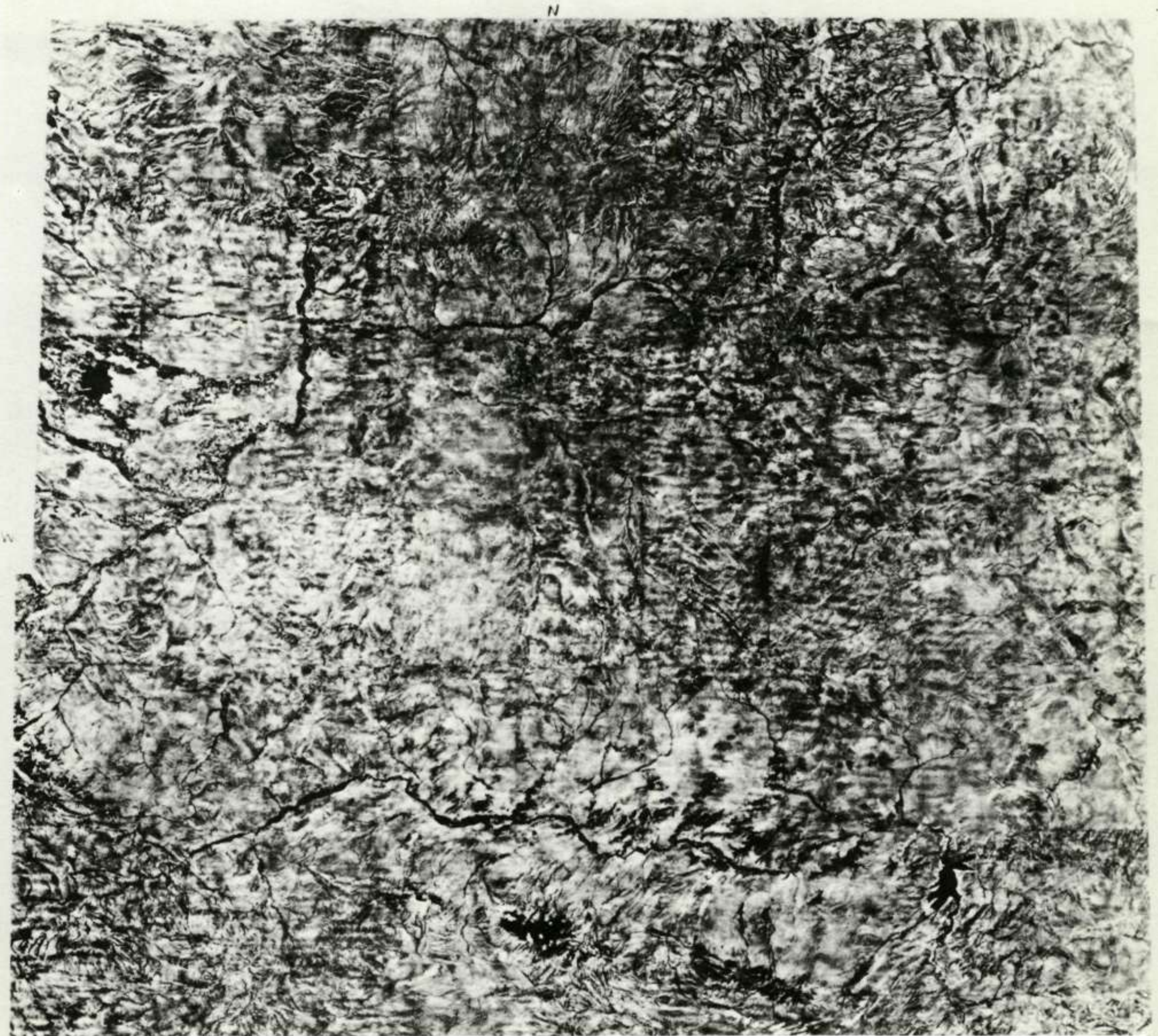

Figure 7b. - Reduction of the Wind River photomosaic to a resolution near 130 meters (estimated with aid of target). Note light and dark horizontal banding in this and other pictures of the scene; this is a form of "noise" apparently introduced during either initial photography or photomosaicing.

b. 

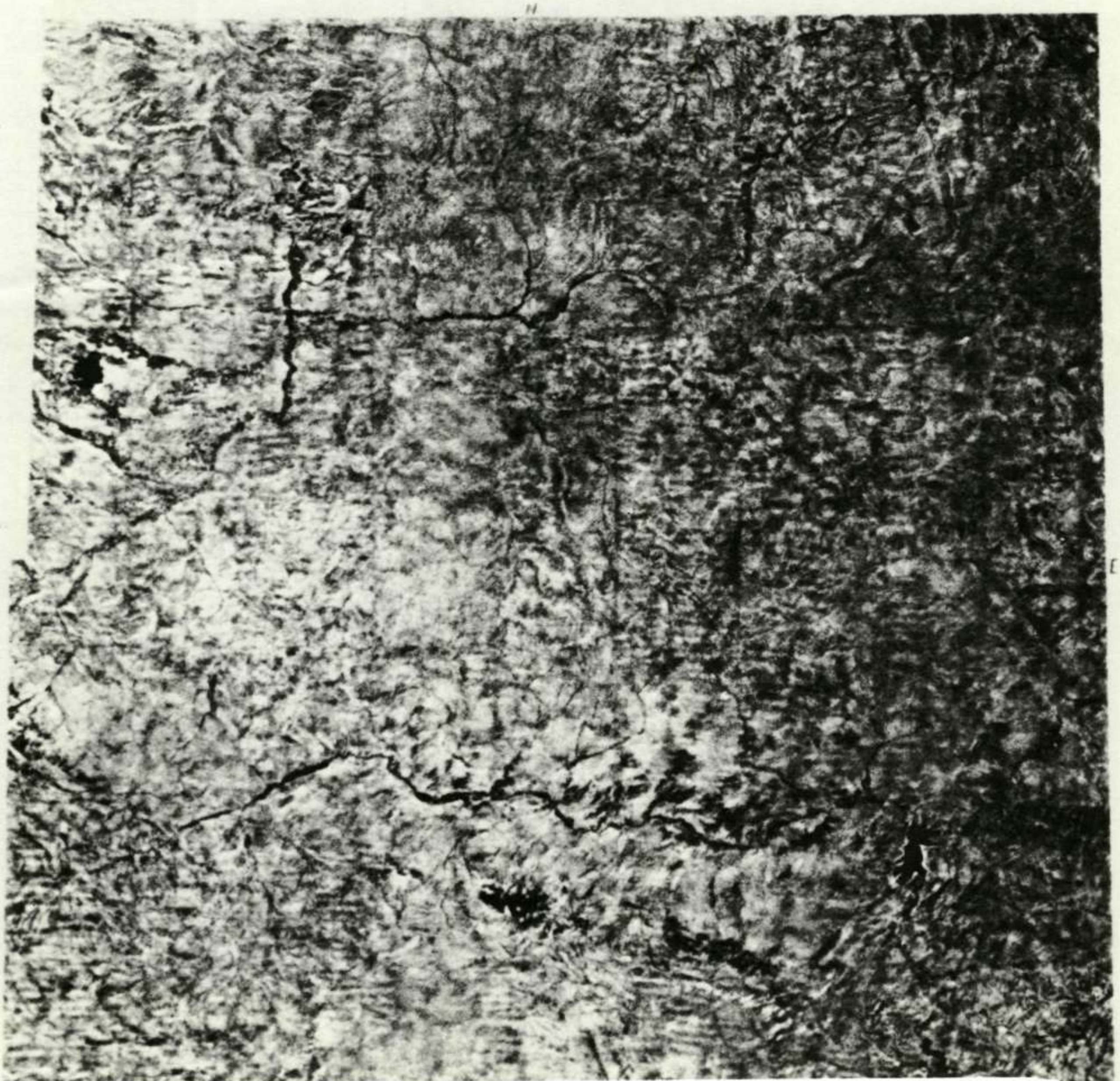

Figure 7c. - Further degradation of the resolution of the original Wind River photomosaic to a value estimated to be 285 meters.

c.

Figure 8. - Uncontrolled photomosaic of central Wyoming (see Figure 6) made from red band photo-frames obtained from a NASA U-2 flight on October 21, 1971. The photomosaic dimensions represent an area approximately 185 km (120 nm) at the base and 160 km (87 nm) from bottom to top. Resolution of original photomosaic is about 18 meters; as printed in this illustration, the resolution is near 75 meters.

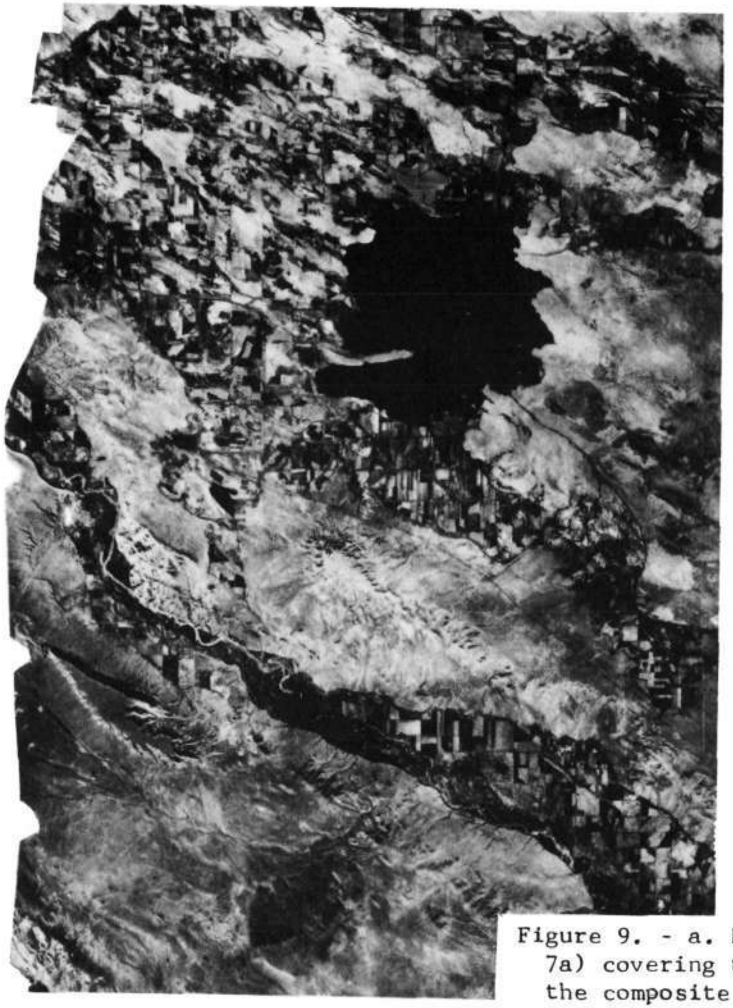

a.~50m

b.~64m

Figure 9. - a. Reproduction of the Aero Service photomosaic (see Figure 7a) covering the region around Ocean Lake, Wyoming (upper left edge of the composite photomosaic). Vertical dimension of photo is equivalent to 25 km on the ground; b. A red band U-2 photo that includes Ocean Lake and its surroundings. This and succeeding photos of Ocean Lake have been degraded by the technique described in the text. Stated resolutions refer to images as printed.

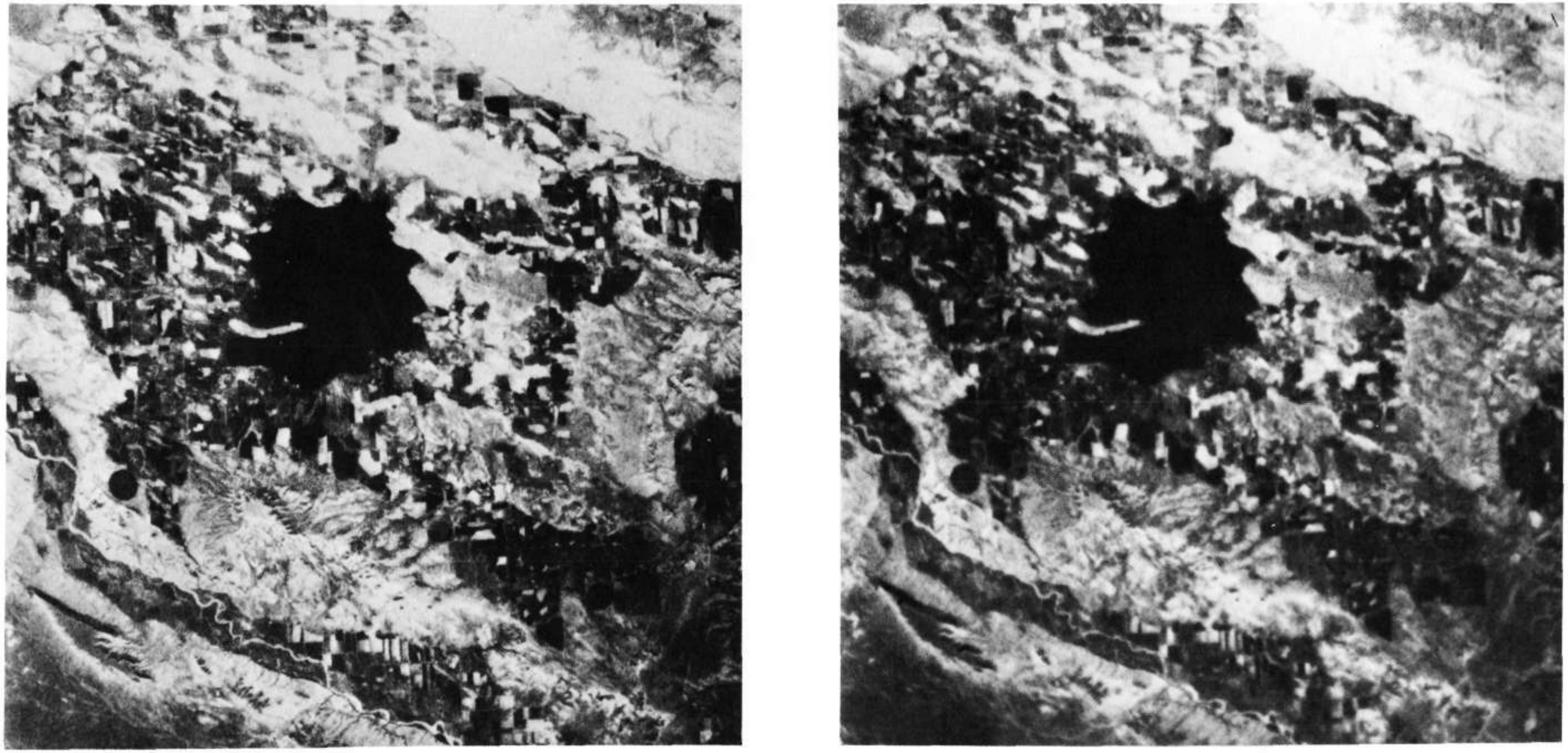

a. ~120m   b. ~260m

Figure 10. - a. U-2 photo of Ocean Lake region with resolution degraded to 120 meters; b. Same scene with resolution now at 260 meters.

a. Green

b. Red

c. IR

Figure 11. - U-2 photographs of the Ocean Lake, Wyoming region as imaged on the October 21, 1971 flight. a. Green band; b. Red band; c. IR band. See text for discussion of principal features in each multispectral image.

a. Green

b. Red

c. IR

Figure 12. - U-2 photographs of area east of Split Rock and north of Lamont in south-central Wyoming (see third photo from right along base of Figure 8) a. Green band; b. Red band; c. IR band. Edge of Ferris Mountains visible at lower left corner. The Sweetwater River crosses from left to right and part of the Granite Mountains (note joints) appear above the river.

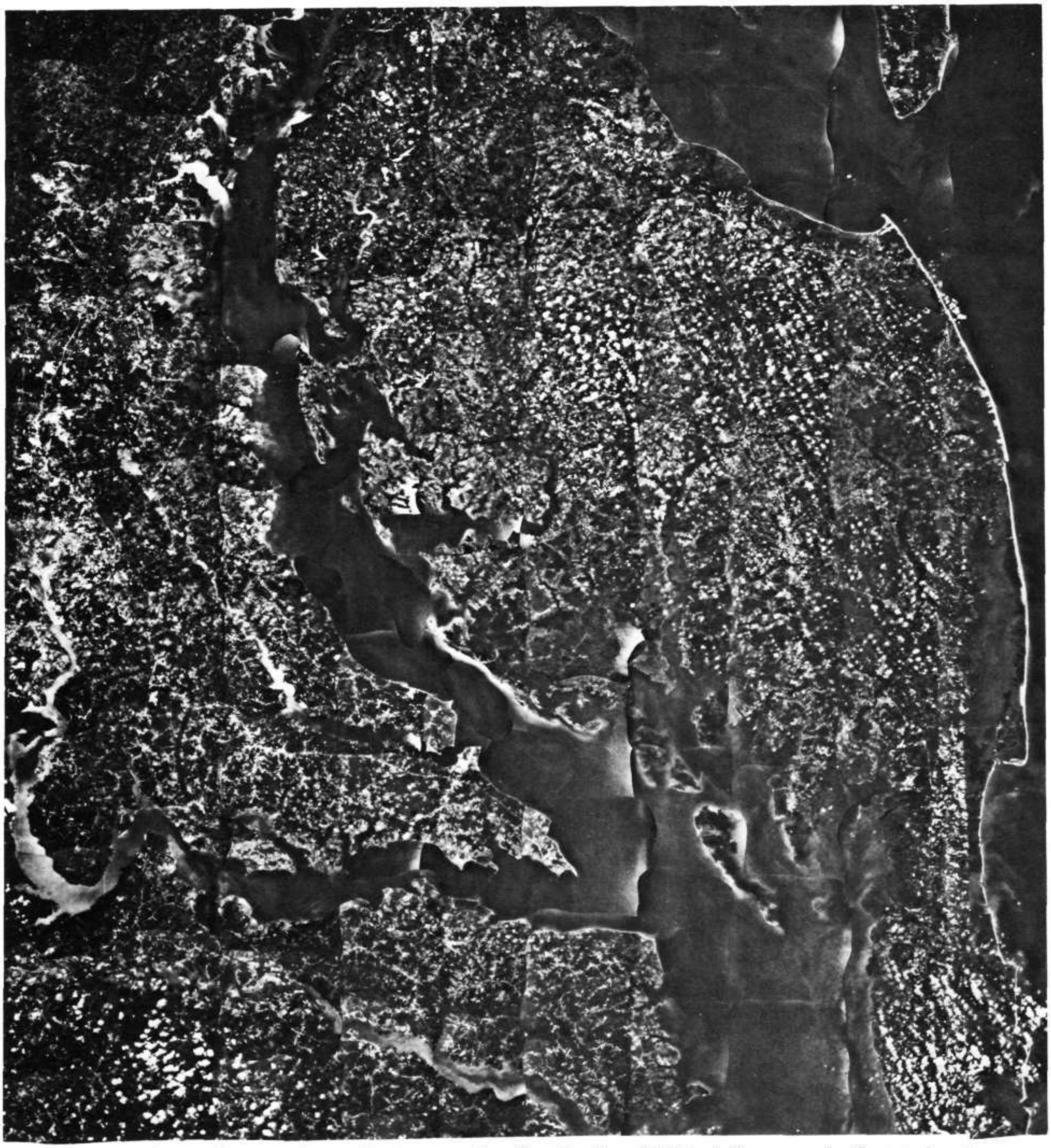

Figure 13. - Composite photomosaic (made by Allied Research Corp.) of the Chesapeake Bay region, using individual frames (red band) obtained from the September 15, 1971 U-2 flight from NASA Wallops Island. Note Washington, D.C. near center left edge; Cape May appears at the upper right corner. See text for equivalent ground dimensions. Resolution in this reduced version estimated to be approximately 60 meters.

a. Green

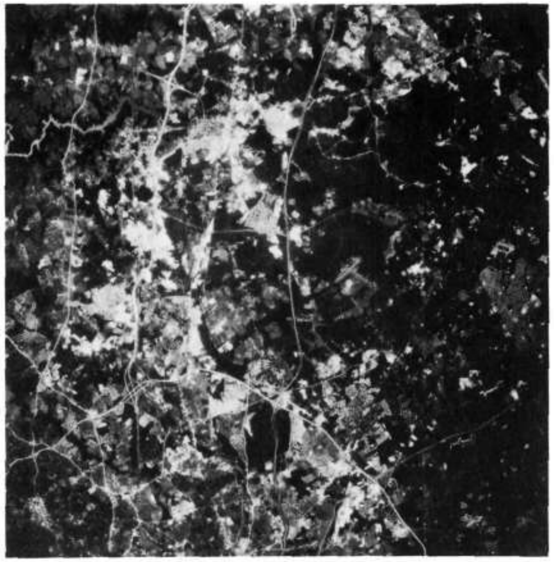

b. Red

c. IR

Figure 14. - Three multiband frames (a. Green; b. Red; c. IR) obtained during the U-2 flight of September 15, 1971, showing an area northeast of Washington D.C. (near center left edge of Figure 13). The Washigton Beltway (appearing as part of a loop) is seen in the lower left and center; the Washington-Baltimore Parkway runs through the center, bottom to top. The community of Belair (Bowie) is shown at the right center edge. See text for discussion of differences indicated in the band images.

a.   b.

Figure 15. - a. A portion of the red band frame (September 15, 1971 U-2 flight) showing a part of the Choptank River estuary near its mouth at Chesapeake Bay, the town of Cambridge, and the farmland along Highway 50 running north (photo appears just above and left of the center of Figure 13); b. The same scene rendered in false color IR by combining the Green, Red, and IR images on a color additive viewer (see text).

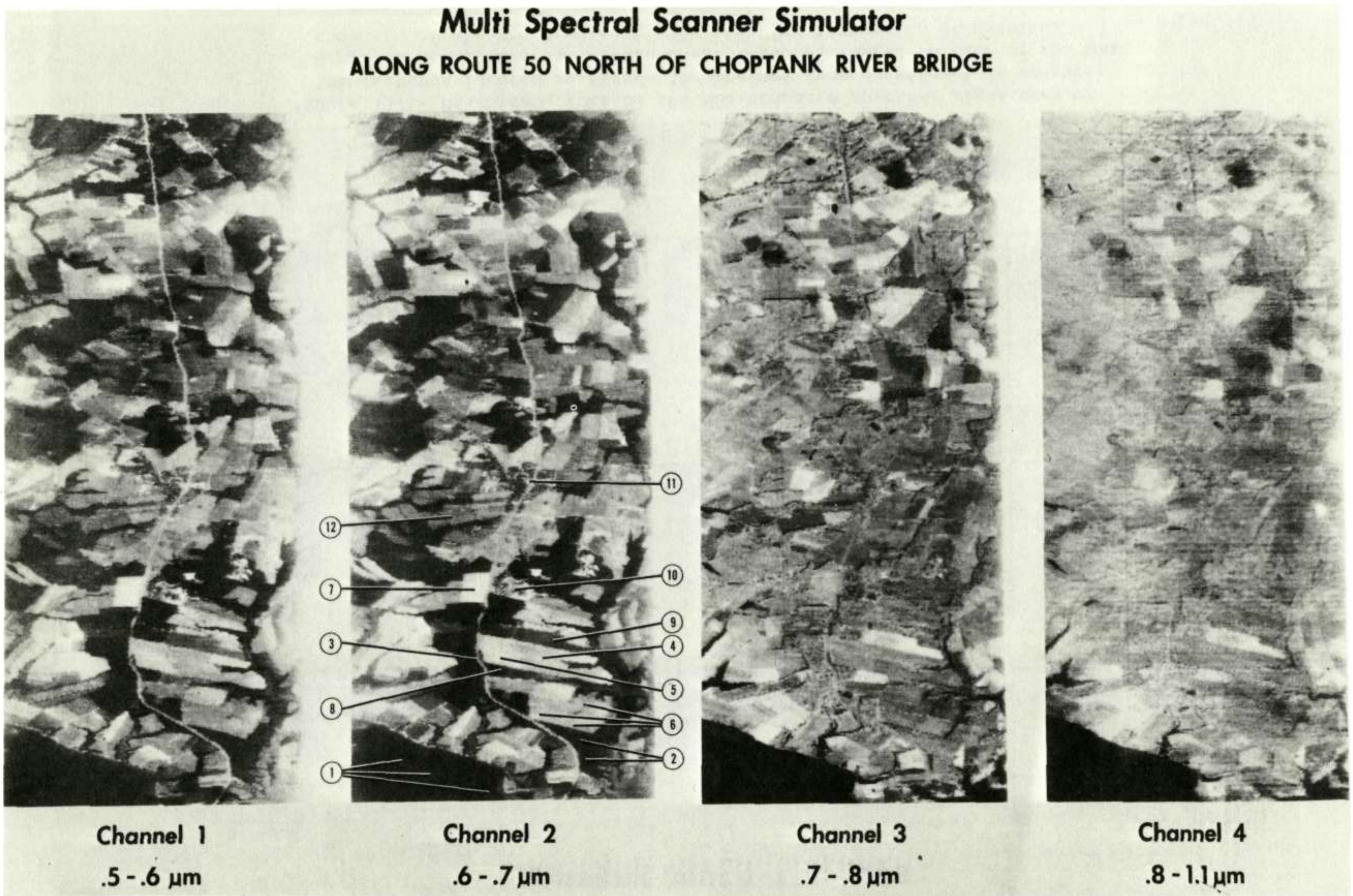

Figure 16.-A segment of the farmland along Highway 50 north of the Choptank River bridge (see Figure 15) as imaged in each of four channels by a prototype ERTS multispectral scanner (MSS) flown on a DC-3 in the fall of 1971. The numbers associated with the channel 2 image refer to various agricultural fields and other features identified in Figure 17.

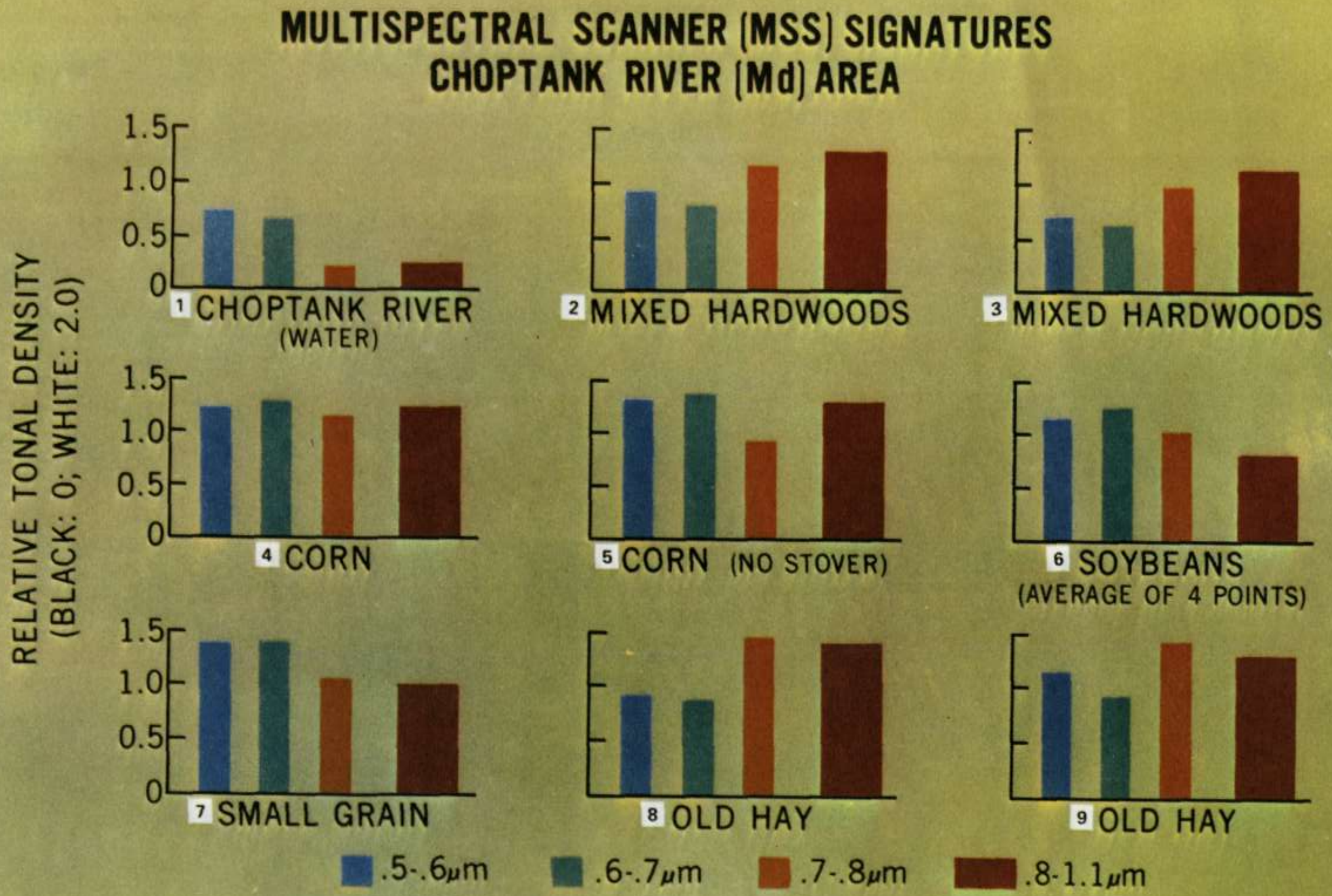

Figure 17. - Histogram plots of the MSS-produced spectral signatures of the features located in Figure 16 obtained from densitometric measurements of selected areas within these features imaged in each of the four channels of the MSS simulator. See text for discussion of results.

a. Green

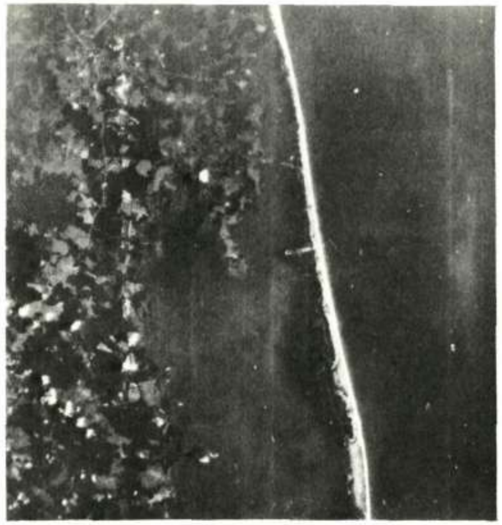

b. Red

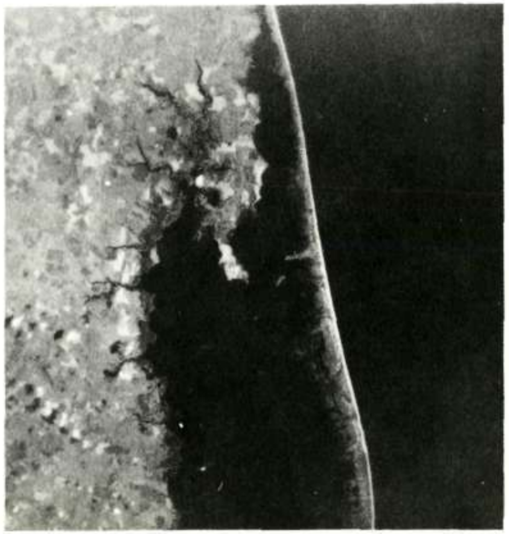

c. IR

Figure 18. - A section along the Atlantic Ocean coastline of Maryland, south of Ocean City, showing the northern end of Assateague Island and Chincoteague Bay. This set of U-2 multiband photos (a. Green; b. Red; c. IR) from the September 15, 1971 flight appears just above the center right edge of Figure 13.

Multi Spectral Scanner Simulator

ASSATEAGUE ISLAND, 14 OCT. 1971

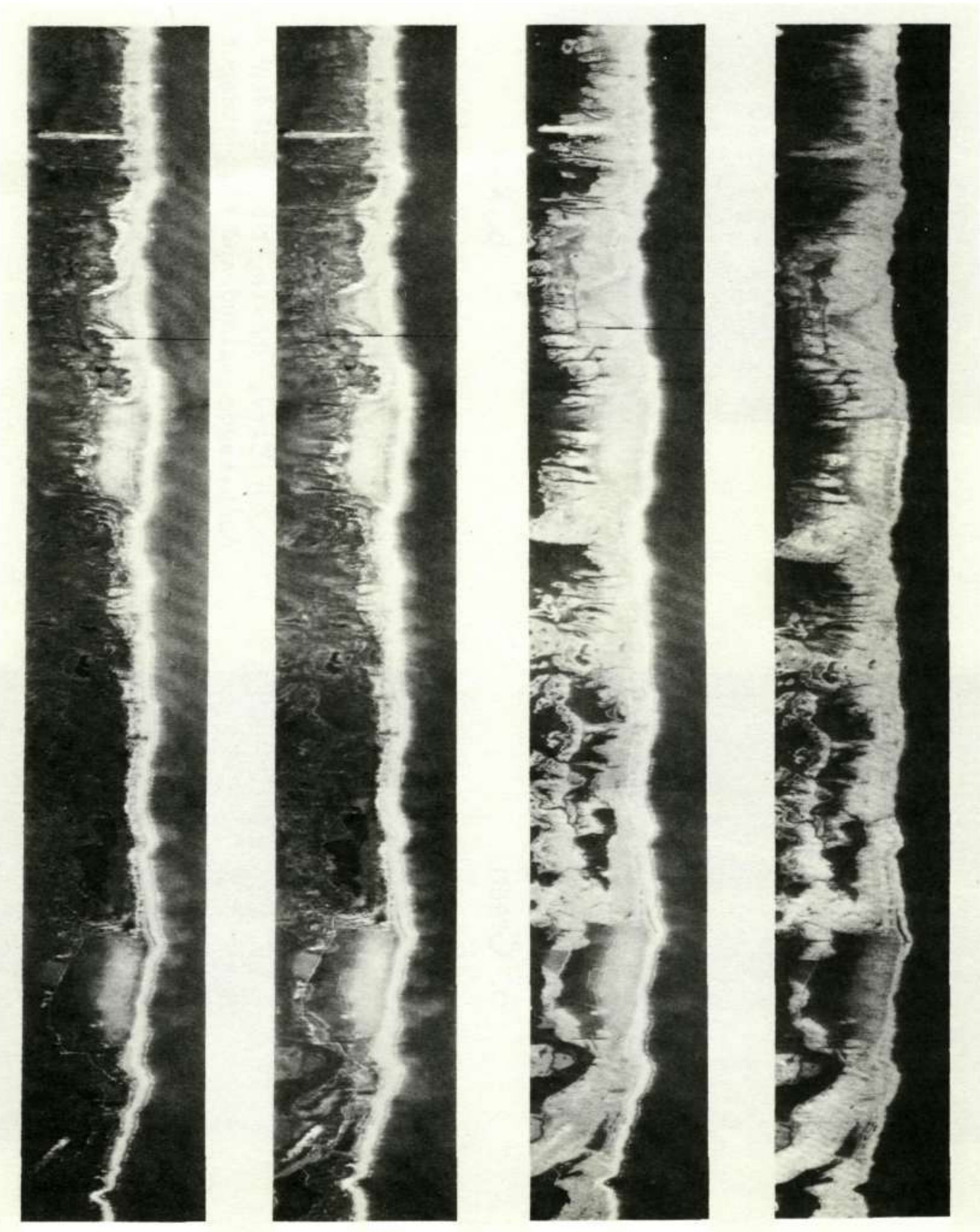

Channel 1	Channel 2	Channel 3	Channel 4
.5 - .6 μm	.6 - .7 μm	.7 - .8 μm	.8 - 1.1 μm

Figure 19. - Images made from the four channel data obtained by the multi-spectral channel simulator during a flight over the Assateague Island offshore bar. The top half of each image corresponds to the lower portion of the island shown in Figure 18.